MATHEMATICAL AND PHYSICAL MODELLING OF STEEL FLOW AND SOLIDIFICATION IN TWIN ROLL / HORIZONTAL BELT THIN STRIP CASTING MACHINES

R.I.L. Guthrie[1], R.P. Tavares[2]

1. McGill Metals Processing Centre, McGill University, 3610 University Street, Montreal, Quebec, Canada, H3A 2A7
2. Associate Professor, Universidade Federal de Minas Gerais, Brasil, Doctoral Candidate, McGill University

ABSTRACT

Near-net-shape casting technology is one of the most important research areas in the iron and steel industry today. Driving forces for the development of this technology include a reduction in the number of operations needed for conventionally produced strip. This is especially true of hot rolling operations. The consequent reduction in investment cost when considering new industrial facilities, makes near-net-shape casting operations extremely attractive from a commercial standpoint.

Various processes for near-net-shape casting of steel are currently being developed around the world. Of these processes, twin-roll casting machines represent a major area of concentration. We believe that one of the main issues concerning the design of twin-roll casters is the metal delivery system and its effect on the homogeneity of solid shell formation, segregation and surface quality.

In the present work, computational fluid dynamics has been used to study different metal delivery systems for twin-roll casting (TRC) and horizontal belt casting (HBC) operations. The METFLO code has been adapted to simulate three dimensional turbulent fluid flows, heat transfer and solidification in these types of machines. The enthalpy-porosity technique was used to couple fluid flow and solidification phenomena. Two configurations for metal delivery system have been studied to date for TRC; one is a conventional tubular nozzle with horizontal outlets in the directions of the side dams. The other is a slot nozzle with a vertical inlet stream.

These simulations have been applied to a pilot caster being studied in Canada, with a roll radius of 0.30 m, producing steel strips with thicknesses ranging from 4 to 7 mm, at relatively low roll speeds ranging between 4 and 12 m/min. Different positions and penetrations of the nozzles in the liquid pool have also been analyzed. It has been shown that a tubular nozzle leads to the formation of a non-uniform solid shell along the roll width. In both configurations, a thicker solid shell is formed close to the roll edges, due to the presence of the side dams.

In the case of horizontal belt casting (HBC), computations have been made for an extended nozzle metal delivery system, and preliminary water modelling tests carried out to confirm the flow delivery concepts proposed. In addition, instantaneous heat flux measurements to simulated belt substrates have been performed for the horizontal casting of aluminum strip that show somewhat similar characteristics to those measured for steel in the pilot TRC, in terms of transient peaks and decays.

1. INTRODUCTION

Fluid dynamics, or mechanics, enters into many aspects of metallurgical processing operations involved in the extraction, refining and casting of ferrous and non-ferrous melts. The transport of heat, or mass, or particles, is often associated with such flows. In ironmaking, for example, optimizing gas flows through the burden of a blast furnace is a key factor in assuring high productivity and good gas utilization by the sinter, or pellets, within the burden. Similarly, mixing rates of "raw" liquid steel in a furnace, or in a ladle during alloy additions, play key roles in optimizing a steel's chemistry and in assuring chemical and thermal homogeneity. Equivalent examples can be quoted for the importance of fluid dynamics for the non-ferrous industries, such as the successes achieved in the field of magneto-hydrodynamics for the production and casting aluminum. Fluid mechanics even enters the field of solidification, in that steel and slag flows within the liquid sump of a casting machine help

determine the quality of the final solidified product, in terms of cast microstructure, macro-segregation, the amounts of entrapped inclusions, and even surface characteristics of the solidified products.

Thus, near net shape casting of steel strip has been under intense investigation and development over the past 20 years. Over that time period, at least 50 casting facilities have been reported built. Only three have been based on belt technology. The remainder are either single-roll casters (e.g., 10) or, far more commonly, twin-roll casters, as first proposed by Sir Henry Bessemer in an 1857 patent. This "holy grail" has been pursued for some 140 years.

2. THIN STRIP CASTING OF STEELS

Thin-strip casting via a conventional oscillating-mould type of technology with liquid core reduction became a commercial reality in Arvedi Group's Acciaieri ISP de Cremona Sri steel works near Milan, Italy. Using the In-line Strip Production technology developed by Mannesmann Demag AG, annual rates of ~ 500,000 tpy of 3 mm gauge, high-grade alloyed and unalloyed carbon and stainless steels are now being produced on a line just 175.3 meters (570 ft) long. However, conventional wisdom foresees frictionless moulds as being required to meet the high exit velocities needed from such machines. Thus, Figure 1 presents a plot of the flow velocity of material out of slab, thin slab, and strip casting machines, versus exit gauge, needed to maintain iso-productivity levels within reach of current slab-caster practices (i.e., ~ 100-150 tonnes/hr per meter width). The various operations noted represent a sample of work recently carried out. [1] One will see from Figure 1 that strip exit velocities in the order of 60 meters per minute and exit gauges of 4 mm are required to maintain productivity levels equivalent to modern-day continuous slab-casting machines.

Twin roll casting of steel is now a commercial fact at the Nippon Steel Corporation. There, stainless steel grades of excellent quality have been successfully and routinely produced at their Hikari Steel Works, using a commercial (10 ton) twin-roll caster fitted with 1.2 m dia rolls. [2] The importance of high rolling speeds (~ 1 m/s) for good surface quality and for minimizing longitudinal cracking problems caused by surface waves, together with the need for intelligent inclusions engineering for the nucleation of a fine ferritic structure, was recently emphasized. [3]

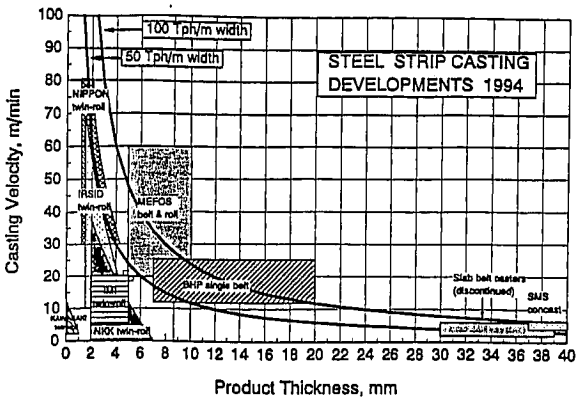

Fig 1. Summary of the projected productivity of near net shape steel caster programmes as reported in the literature.

While many similar twin-roll caster programs (e.g., 60) are either in progress or already completed, there currently exists only one pilot-scale program dealing with an alternative approach for high-volume *thin-strip* production, and this is at MEFOS, Lulea, Sweden. The direct-steel-casting (DSC) concept involves a horizontal-belt caster. The major advantage of such a technology is that one has available an infinite radius roll (i.e., flat belt), that can theoretically be designed to accommodate any level of production and strip thickness reasonably called for. One of its major shortcomings has been the problem of maintaining belt flatness, but these difficulties are largely resolved, to the point that variations to less than $\pm$ 0.1 mm are now confidently expected. [4]

Figure 2 provides details on the length of such a direct steel caster required to produce a given tonnage of steel as a function of the percent volume solidified within an extended nozzle delivery system. [5] These computations assume a typical solidification rate constant of 20 mm/min$^{1/2}$, according to the relation

$$\delta_s = k\sqrt{t}$$

where:
δ_s = thickness of solidified shell (mm);
t = contact time between steel melt and cold substrate (mm); and,
k = solidification rate constant (mm/min$^{1/2}$).

For instance, assuming one wishes to produce 8 mm final thickness with a 4 mm thick substrate

(i.e., 50% solidified) exiting the extended nozzle delivery system, then a contact length (see ordinate) of about 1.06 m would be needed at 100 tph/m width, or about 0.55 m at 50 tph/m width.

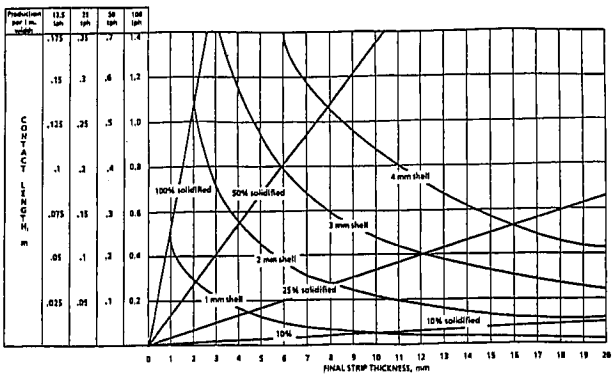

Fig 2. Relation between mould contact length, find strip thickness and percent of metal solidified at nozzle exit, for various production rates.

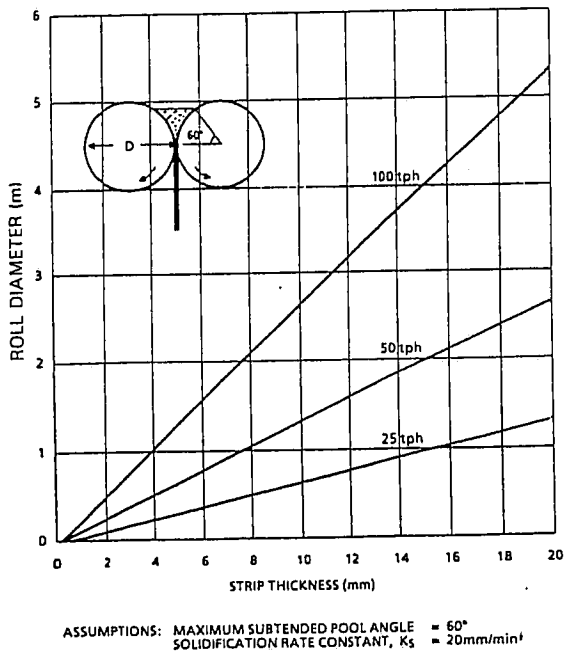

Fig 3. Plot of roll diameter (m) versus thickness of solidified strip (mm) at the roll nip for various levels of productivity (tonnes per hour).

Figure 3 shows the results of similar computations for a twin-roll caster. [6] Again, one can readily demonstrate that a twin-roll caster would require working roll diameters in the order of 2.6 meters (or 9 ft) to produce 10 mm thick strip (2 x 5 mm) at the roll nip, if it were designed to match current slab caster operations. [1] Such massive roll diameters seem unlikely, although attempts at such were made at the turn of the 20th century. The example to produce 10 mm thick strip was chosen as this would allow for subsequent hot-rolling operations aimed at improved properties with 1997 AD grades of steel.

However, such simple correlations ignore the more intricate details of fluid flow, heat and mass transfer within the mould regions of such strip-caster systems, and are therefore only of first-order accuracy. This paper is also concerned with more detailed predictions of flows and solidification patterns within the mould regions of twin-roll and direct-steel-casting machines.

3. NUMERICAL MODELLING METHOD

3.1 Mathematical Formulation

A steady-state three dimensional fluid flow, heat transfer and solidification model has been developed and applied to the twin-roll casting process for steel. In this model, the turbulent form of the Navier-Stokes equation is fully coupled with a differential energy balance equation that takes solidification into account. For turbulence, a low-Reynolds number form of the k-ε model has been used. For enthalpy, the approach suggested by Bennon and Incropera [7] was adopted.

The conservation equations for each of the dependent variables (u, v and w velocities in the x, y and z directions, respectively, k, ε and enthalpy, h) can be written in the general form:

$$\frac{\partial}{\partial x}(\rho u\phi)+\frac{\partial}{\partial y}(\rho v\phi)+\frac{\partial}{\partial z}(\rho w\phi)= \frac{\partial}{\partial x}\left(\Gamma\phi\frac{\partial\phi}{\partial x}\right)+\frac{\partial}{\partial y}\left(\Gamma\phi\frac{\partial\phi}{\partial y}\right)+ \frac{\partial}{\partial z}\left(\Gamma\phi\frac{\partial\phi}{\partial z}\right)+S_\phi\,(x,y,z) \qquad (1)$$

where ρ is the density, ϕ represents the dependent variable and Γ_ϕ and S_ϕ are its diffusion coefficient and source term, respectively.

3.2 Turbulent Flow

One point of concern when turbulent models are used is related to the boundary condition adopted for the velocities and temperature. A popular approach to computing convective transfer rates in turbulent flow is to assume that close to the solid-liquid interface, but sufficiently away from it for the effects of molecular transport to be negligible, the velocity and temperatures profiles are given by the so-called universal logarithmic laws. In this case, instead of applying boundary conditions at the solid-liquid interface, the values of velocity and temperature are simply matched to the ones given by the logarithmic laws in a point away from the interface. This approach is called the wall-function method. The limitation of this method is that not all boundary layers possess a turbulence structure near the solid-liquid interface that conforms to the pattern associated with the logarithmic laws. This is particularly true in problems that involve solidification, in which the solid-liquid interface normally has a complex morphology, usually with dendrites, whose spacings depend on the cooling rate. This virtually excludes the possibility of applying the wall function in solidification problems, other than those involving planar freezing.

To circumvent this shortcoming, a low-Reynolds number formulation was adopted. In this case, the momentum and energy equations, coupled with expressions for k and ε, were solved up the solid-liquid interface. Other terms, related to the boundary conditions at this interface, were added to the k and ε equations and a new function, f_R, introduced into the equation for evaluating the turbulent viscosity:

$$\mu_T = f_R \, C_\mu \, \rho \frac{k^2}{\varepsilon} \qquad (2)$$

where:
μ_T = turbulent viscosity;
C_μ = constant;
k = kinetic energy of turbulence;
ε = dissipation rate of kinetic energy.

Different low-Reynolds number models have been proposed in the literature [8]. Recently, those developed by Launder and Sharma and Launder and Jones were applied to solidification in continuous casting systems by Aboutalebi and co-workers [9] and their predictions agreed well with experimental results. In the present work, the same formulation was used:

$$f_R = \exp\left(\frac{-3.4}{\left(1+\frac{R_t}{50}\right)^2}\right) \qquad (3)$$

where Re_t is the turbulent Reynolds number given by:

$$Re_t = \frac{\rho k^2}{\mu \varepsilon} \qquad (4)$$

where μ is the laminar or molecular viscosity.
As seen, the function f_R tends to unity as the turbulent Reynolds number increases but becomes much smaller than unity with a decrease in Re_t. This consequently increases the importance of the laminar viscosity at points close to the solid-liquid interface, in keeping with physical reality.

3.3 Solidification

To account for solidification effects, several changes were introduced. In the momentum equations, an additional source term was incorporated. Based on the work of Poirier[10], it was assumed that the columnar mushy zone behaves like a porous medium and obeys Darcy's equation. Therefore, the form of the additional term is such that it makes the momentum equation reproduce Darcy's equation when the solid fraction increases. The general form of this source term is:

$$S_\phi = \frac{k_o (1-g_l)^2}{(g_l + A)^3} \cdot (\phi - \phi_s) \qquad (5)$$

where:
ϕ = u, v or w velocity;
k_o = morphology constant;
g_l = liquid fraction;
A = small number (just to avoid division by zero, when the liquid fraction goes to zero);
ϕ_s = y or z component of the roll velocity.

The effect of this term on the momentum equations is to require velocities within the mushy zone to gradually approach the corresponding component of the roll velocity, as the liquid fraction decreases. The value of k_o determines the speed of this approach. Numbers in the range of 10^5 to 10^7 have been chosen [11, 12] for the morphology constant. This usually gives results in reasonable agreement with experiments.

An alternative to this approach consists in writing equation (5) in terms of the permeability of the mushy zone. The permeability is inversely

proportional to the morphology constant and several relations have been proposed for its evaluation. One of the most recent was suggested by Schneider and Beckermann. [13] In this formulation, the permeability was expressed as a very complicated function of the liquid fraction and primary and secondary dendrite arm spacings. Two different relations were given according to the direction of flow. This relation shows that the permeability of the mushy zone decreases when the dendrite spacings are smaller, or when the cooling rate is higher. Although this formulation is more appropriate, there still remains significant uncertainty in this kind of expression for permeability, especially for steel.

In the present paper, the morphology constant formulation was adopted, and since the cooling rate in twin-roll casters is very high (dendrite arm spacings between 10 and 40 μm [10]), a value of k_o in the upper limit of the range (10^7) was assumed. In arbitrarily defined areas around the nozzle and close to the side dams, the velocity ϕ_s in equation (5) was set to zero, instead of being the component of the roll velocity. This would make the velocities in those regions approach zero when the solid fraction increases.

To damp turbulent transport inside the mushy zone, the method proposed by Shyy and co-workers [12] was adopted and a correction in the function f_R based on the local liquid fraction, namely,

$$f_\mu = \sqrt{g_1}\, f_R \qquad (6)$$

was introduced. Function f_R is then replaced by f_μ in the evaluation of the turbulent viscosity.

Another important issue in solidification modelling is the release of latent heat and the evaluation of solid, or liquid, fractions. In this work, a simple relation for liquid fraction as a function of enthalpy was used:

where: h = enthalpy of steel at a certain temperature, between *liquidus* and *solidus*

$$g_1 = \frac{h - h_s}{h_1 - h_s} \qquad (7)$$

temperatures;
h_s = enthalpy of steel at the *solidus* temperatures;
h_l = enthalpy of steel at the *liquidus* temperature.

The enthalpy was defined as:

$$h = C_p \left(T - T_{ref}\right) + g_1 \cdot L \qquad (8)$$

where:
C_p = specific heat;
T = temperature;
T_{ref} = reference temperature (arbitrary);
L = latent heat.

This relation was also used by Flint. [11] Formulations based on the lever rule [7, 15] and parabolic functions of temperature [16] have also been proposed. Since solidification in strip casting processes is very fast, it does not seem reasonable to assume equilibrium conditions and in this case the lever rule will not be valid. A more correct evaluation of the liquid fraction in the present model would involve modelling of micro- and macro-segregation in multi-component steel alloys. [13] This would certainly increase, even more, computation times, without changing the basic character of the results.

3.4 Boundary Conditions and Physical Properties

Considering symmetry, only one quarter of the twin-roll caster was studied. For boundary conditions, non-slip conditions were assumed on all solid boundaries, including the roll surface. On the free surface, heat losses by convection and radiation were considered. On the surface of the rolls, an overall heat transfer coefficient was used. Its value was deduced from global heat balances and exit surface temperatures of the strip, as obtained in the pilot caster under investigation. The side dams and the nozzle were considered adiabatic.

The *liquidus* temperature was evaluated as a function of steel composition [17] and the *solidus* was assumed to correspond to the peritectic temperature.

Table I give the physical properties and casting parameters adopted for model runs. All the physical properties were assumed constant.

The algebraic equations were solved using an alternative-direction line-by-line method. To guarantee convergence, under-relaxation was applied to all variables and in the enthalpy source term. It was required that the summation of the residuals of all the equations for each variable be smaller than 0.25 %, in relation to the correspondent inlet quantity, before the numerical

procedure was terminated, and a converged solution assumed.

A non-uniform grid system with 58 x 51 x 20 nodes, covering one quarter of the twin-roll caster, was adopted. Further increases in the number of nodes did not lead to significant changes in the results.

Table I. Physical Properties and Casting Parameters for TRC Model Runs

- Physical properties of low carbon steel:

  density: 7000 kg/m^3
  specific heat: 680 J/kg.K
  heat conductivity: 36 W/m.K
  viscosity: 6.2 x 10^{-3} kg/m.s
  emissivity of the liquid: 0.28
  liquidus temperature: 1524°C
  solidus temperature: 1495°C

- Casting parameters:

  roll diameter: 0.6 m
  roll width: 0.2 m
  pool depth: 0.192 m (40° contact angle)
  casting speed: 4-12 m/min
  strip thickness: 4-7 mm
  overall heat transfer coefficient:
  2000-3000 W/m^2.K
  nozzle:
  - tubular: - penetration 40-50 mm
  - opening (diameter): 16 mm
  - slot: - penetration: 3 cm

3.5 Numerical Procedure

The conservation equations were discretized and solved with our in-house METFLO code. This code gives different choices for the discretization scheme for each variable: upwind, hybrid or power-law scheme.

4. TWIN ROLL CASTING: RESULTS AND DISCUSSION

4.1 Tubular Submerged Entry Nozzle

Figure 4 (4.9) shows the computed velocity field for a tubular nozzle with horizontal delivery ports. The casting speed is 0.188 m/s or 11.3 m/min, and the nozzle's depth of penetration 50 mm. As seen, the flow is quite complex, the horizontal jets moving out towards the side-dams and then back around towards the mid vertical plane of the caster, in twin recirculatory loops. Figure 5 (4.10) gives a view of the surface flows induced by this type of nozzle inlet configuration. As one might expect, hot entering steel loses its superheat and the coldest liquid is to be found along the central surfaces of the rolls, Figure 6 (4.12) leading to more rapid solidification of the advancing steel shell. This is reflected in the uneven solid fractions within the wedge-shaped pool across a horizontal plane 100 mm below the top free surface of the steel, as depicted in Figure 7 (4.13).

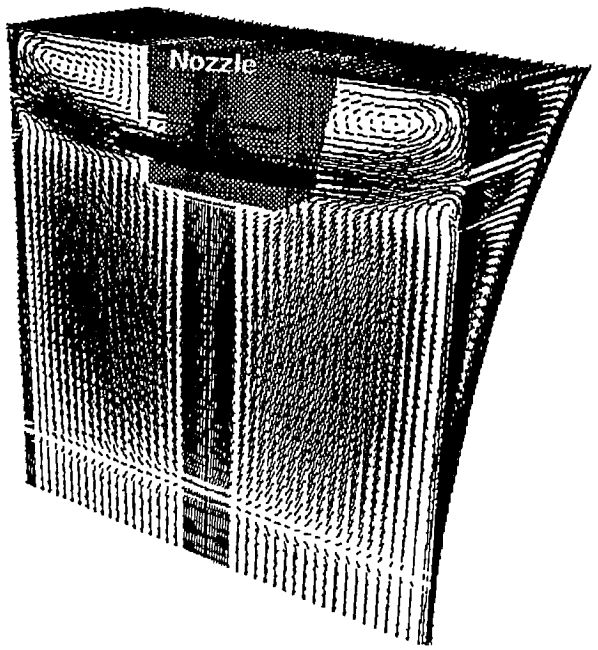

Fig 4. Velocity field with the tubular nozzle with horizontal ports.

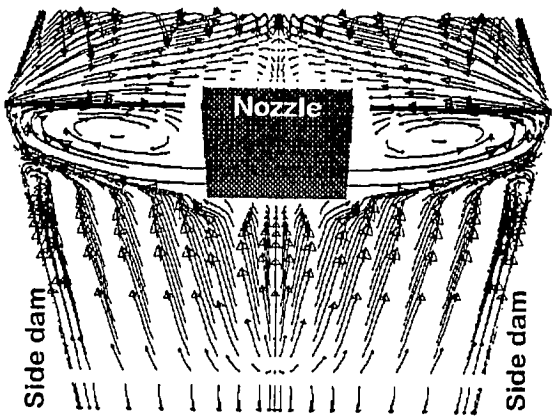

Fig 5. Velocity field with the tubular nozzle. Detail of symmetry plane and top surface.

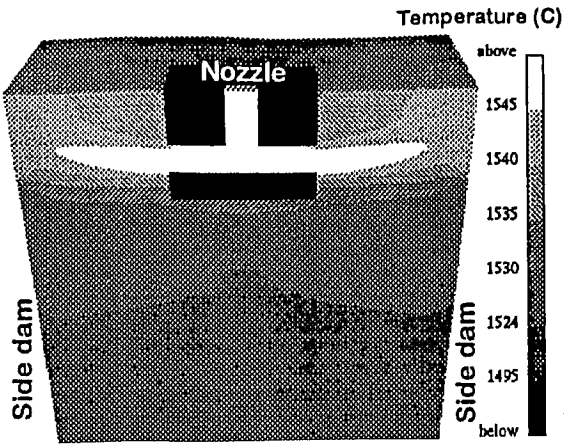

Fig 6. Predicted temperature profile with tubular nozzle.

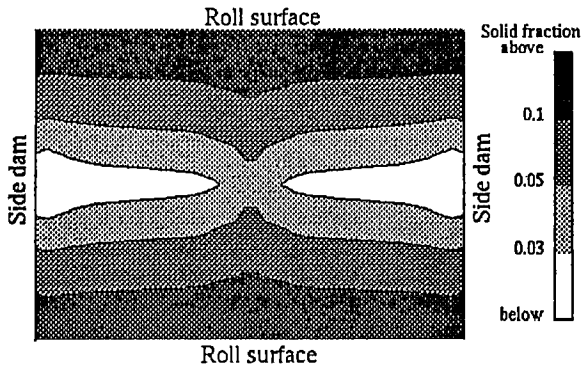

Fig 7. Solid fraction profile at a horizontal plane 100 mm below the top surface. Tubular nozzle.

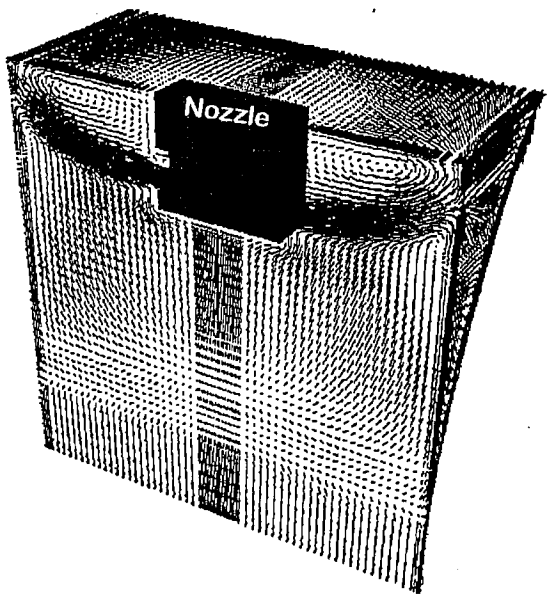

Fig. 8. Velocity field for the full-scale water model with tubular nozzle.

In order to confirm the reliability of the CFD computations physically, a full scale water model of the pilot TRC was constructed, and computations run with a 2 mm thin strip exit port, a roll velocity of 18.8 m/min and a nozzle submergence depth of 50 mm. The computed flow field (in the absence of solidification) is depicted in Figure 8 (4.53). Predictions of a reverse flow region close to the roll exit port (or roll nip) was confirmed through dye tests. Similarly, particle tracers were used to compare flows close to one of the side dams with those predicted, and excellent agreement was found.

4.2 Slot Shaped Submerged Entry Nozzles

In order to investigate the behaviour of slot nozzles with vertically penetrating steel, and to predict their influence on the evenness of the forming shells, a series of computations were carried out to predict the influence of slot nozzle width versus caster width.

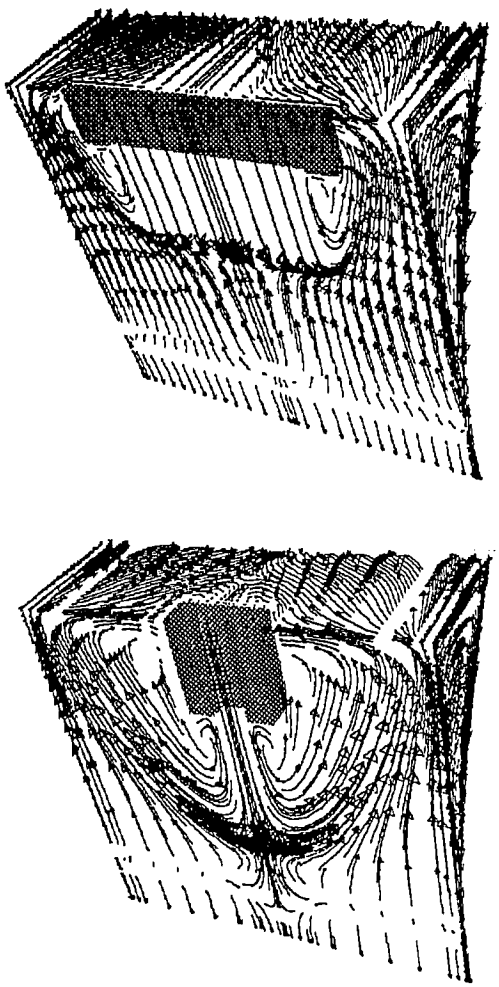

Fig 9. Velocity fields with slot nozzles.
a) 50% of the roll width
b) Tubular vertical nozzle

Figure 9 presents computed flow fields for a vertical slot nozzles of the roll width, and a tubular nozzle respectively, while Figures 10 a, b, and c show corresponding computed solid fraction contours 100 mm below the free surface for these, and a slot nozzle spanning the complete width of the strip.

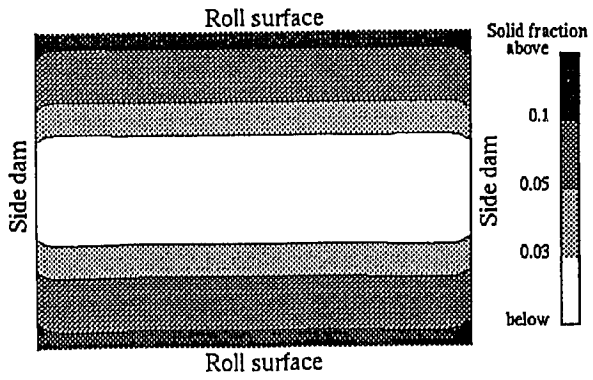

a)

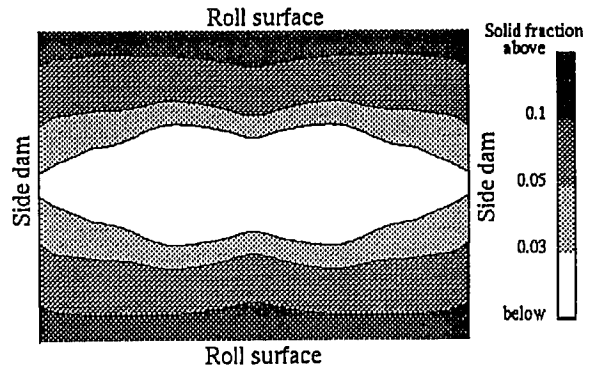

b)

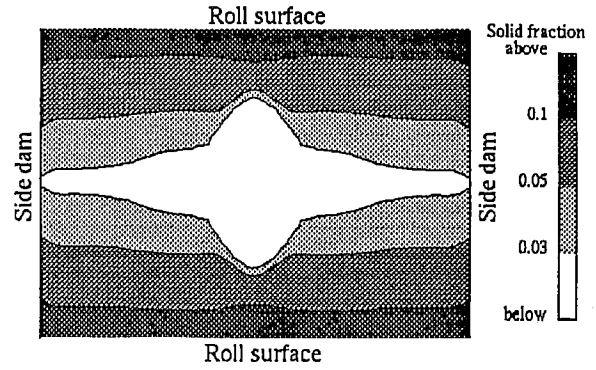

c)

Fig 10. Solid fraction profiles at a horizontal plane 100 mm below the top surface. Slot nozzle.

a) Full width of the roll
b) 50% of the roll width
c) Tubular vertical nozzle

Nozzle penetration for these computations correspond to 30 mm. The slot nozzles themselves were chosen to be 7 mm thick (2.5 mm wall thickness) with a 2 mm thick exit slot. As might be anticipated, a vertical entry slot nozzle equal to the width of the strip being produced gives the best result in terms of thickening shell uniformity since the flow within the TRC becomes essentially two-dimensional in character. One sees that a vertical slot nozzle only 50% of the caster width would probably be inadequate unless some sort of flow modifiers were incorporated into the slot nozzle, or caster pool.

4.3 Heat Fluxes to Substrate Rolls

Notwithstanding the above predictions, one of the key problems in all CFD computations, of course, is to select realistic boundary conditions for heat fluxes. Consequently, three sets of thermocouples were embedded in the sleeve of one of the TRC pilot caster's rolls to assess instantaneous localized heat transfer coefficients across the width of the roll during contact of the roll with molten steel.

Using an in-house inverse heat transfer code [18], local heat fluxes were deduced as a function of contact time. One such result is shown in Figure 11 where a sharp increase is followed by a decrease.

In another result (Figure 12), the first peak is followed by a second peak. In the case of a twin roll caster, such variations are a consequence of an interplay of different factors, such as the presence of an entrapped air film between the roll and the thin solidified shell, thermal expansion of the rolls, metallostatic pressure, solidification, shrinkage, and intermeshing of the two solidifying strips. Additionally, the roughness and thermal properties of the coatings applied to the role play a significant roll in determining actual heat fluxes.

In the simulations reported, these complicating factors were avoided by using uniform overall heat transfer calculations. Table 1 provides details of the physical properties of low carbon steel and the casting parameters associated with our computations. This approach was justified on the grounds that the development of the shell profile was a major objective of this work, and that our model was not built to consider hot metal deformation processes.

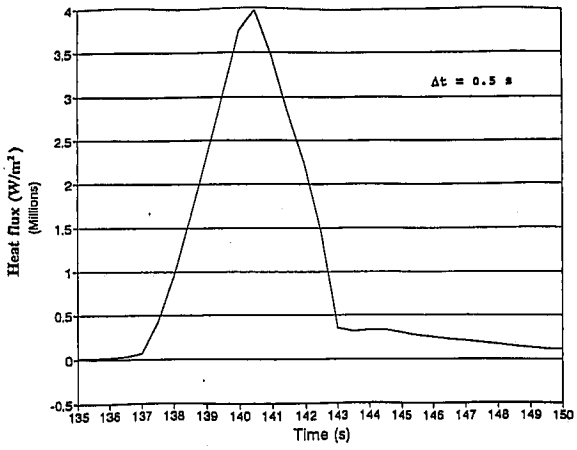

Fig 11. Variation of the heat fluxes during the contact time. Low casting speed and thick strips (6.5 mm) (0.066 m/s).

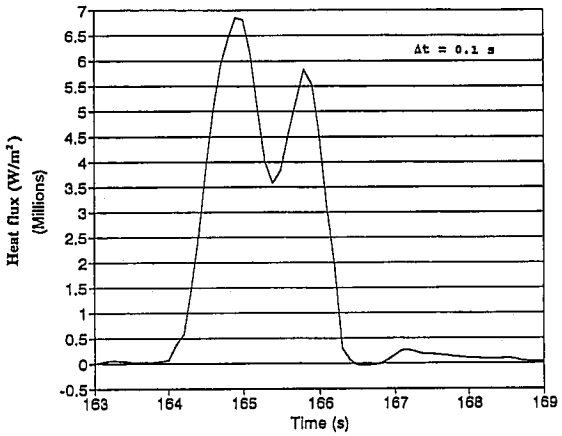

Fig 12. Heat fluxes during the contact time. High casting speed (0.13 m/s) and thin strips (4mm).

5. HORIZONTAL STRIP CASTING

Figures 13 a and b illustrate the horizontal-belt strip-casting concept independently proposed by one of the present authors [5,6] and by K. Schwaerdtfeger and Mannesmann Demag Huttentechnik (MDH), now in conjunction with MEFOS and a consortium of companies and universities. [4] The drawing is schematic, in that a single endless horizontal belt runs between two rollers, its bottom surface being water-cooled, and held under negative gauge pressure to promote belt flatness. This, together with preheating the cold side panels, or frames, not exposed to molten steel from the metal-delivery system, and pre-tensioning that part exposed to hot metal, can regulate belt flatness to better than 0.1 mm.

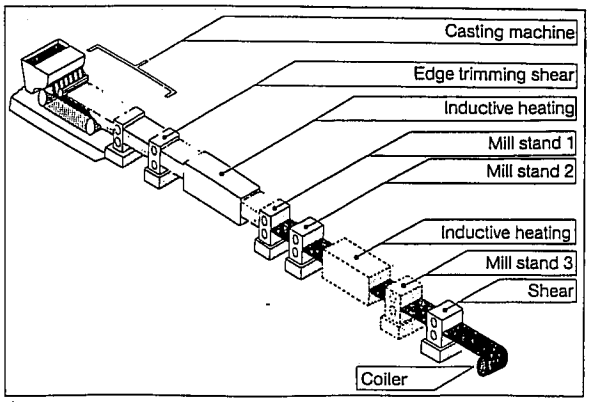

a)

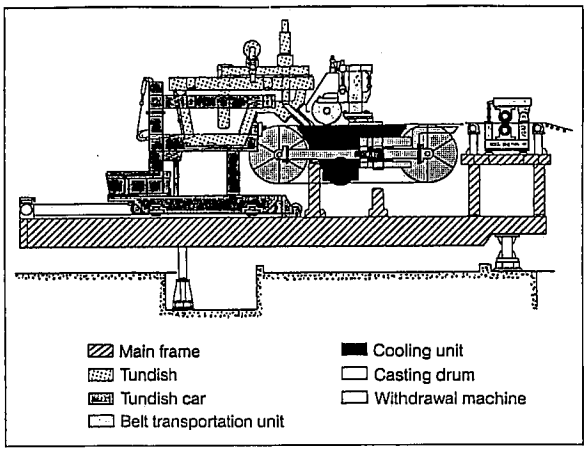

b)

Fig. 13 a) Direct strip production; schematic view
b) Direct strip production; schematic view of the pilot caster

5.1 Metal Delivery Systems

In the Mannesmann metal-delivery method (Figure 14), a low-pressure metal-feeding system is used, in order to restrict the natural head velocity, $U\left(=\sqrt{2gh}\right)$, of steel exiting the nozzle. The system, in principle, can achieve low-turbulence conditions but is complicated to handle. [4] It is divided into two (filling and low-pressure) sections. The tundish is filled to a certain level, negative pressure is applied to generate the casting head required, and the stopper rod raised (opened). By this means, the relative velocities of the entering steel can be adjusted to belt velocity, so as to minimize turbulence. The control of gauge thickness, inert gas shrouding, and non-pressurized delivery of metal to the initial point of contact would seem to be problem areas for such a design.

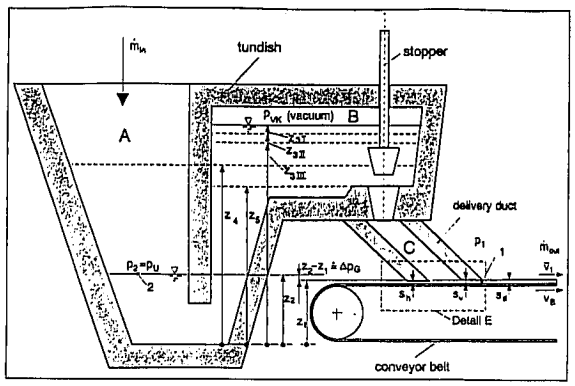

Fig 14. Schematic diagram of a low pressure liquid steel feeding system with adjustable casting pressure Δp_G

A tube feeding system was developed more recently at MEFOS. While the technique generates higher turbulence at the point of transfer onto the belt, it is easier to preheat and operate. The casting level in the feed tube is kept constant by means of laser measurements of the meniscus with feedback control to the stopper rod. This method of metal feeding is reminiscent of the approach used by British Steel Corporation's thin-slab casting project, in that the metal flows over weirs.

An alternative approach to metal feeding, employing the principle of an extended nozzle delivery system, in conjunction with the MEFOS feed tube, is shown schematically in Figure 15. This system, which incorporates an extended flow modifier (e.g., porous reticulate medium) has the advantage that metal is delivered at *low velocity*, normal to the cooling substrate (belt), assuring even, smooth flow of metal within the mould region, even though the belt and substrate typically exit the mould at speeds of 1 m/s or more.

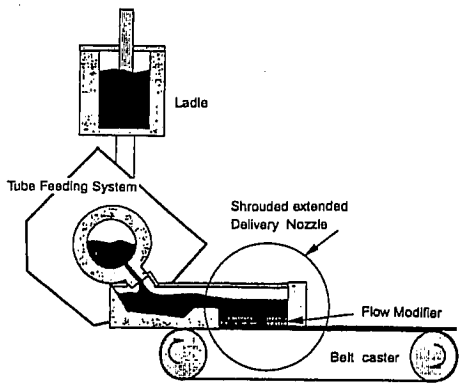

Fig 15. Schematic of the extended-nozzle metal-delivery system.

Furthermore, the freezing substrate is pressurized by the natural head of steel above the mould region, for enhanced surface quality and improved heat transfer.

In modelling this system, the machine parameters and physical properties corresponding in part to the pilot-scale equipment built by Hazelett and purchased by BHP (Australia) to test this concept, were adopted. Unfortunately, this program had to be curtailed prematurely to concentrate on Project M involving a twin roll caster. However, Table 2 provides all the relevant parameters used for the numerical computations now presented. As seen, the reservoir height was 57 mm, the exit gap from the caster 10 mm, the extended nozzle delivery 200 mm long, while the mass flow of low-carbon steel was 227 tonnes/hr per meter width of strip.

Table II. Physical Constants and System Variables

Roll diameter	Infinite
Pool depth	5.7 cm
Casting speed	0.9 m/s
Extended pool length	20 cm
Strip thickness	10 mm
Refractory wall thickness	3 cm
Flowrate for a 15 cm width	9.45 kg/s
Material	Low-carbon steel
Liquidus temperature, T_l	1535°C
Solidus temperature, T_S	1492°C
Viscosity	0.007 x 100 kg/(m s)
Density	7,000 kg/m^3
Latent heat	283.6 kJ/kg
Heat Capacity, c_P, liquid steel	824.1 J/kg · K
Heat Capacity, c_P, solid steel	716.2 J/kg · K
Thermal conductivity, liquid steel, k_l	30.5 x 7 W/m · K
Thermal conductivity, solid steel, k_S	80.0 W/m · K
Thermal conductivity, refractory steel, k_r	1.4 W/m · K
Emissivity, steel	0.28
Emissivity, refractory	0.8

5.2 Computations

In modelling the extended nozzle system, the specific governing equations for fully coupled energy and fluid flow, using an enthalpy-porosity scheme are fully described in a previous paper. [19] However, in brief, the entry wall of the extended nozzle system shown in Figure 16 was taken to be adiabatic, while the exit wall of the extended

nozzle was treated as a conjugate solid body within the computational domain. Radiation from the exiting strip was assumed, while a varying heat flux along the chilled substrate was calculated using a varying heat transfer coefficient. At the initial region of metal contact with the belt, h was taken to be 10 kW/m^{2}K. Once the forming strip had exited, the lower value of 1.4 KW/m^{2}K was adopted. These numbers represent best estimates based on the literature and need to be confirmed in practice. However, corresponding heat flux data (Q = 15 to 7 MW/m^2, L = 0 to 80 mm; Q = 3.5 MW/m^2, L = 90 to 230 mm; Q = 2 MW/m^2, L = 2300 to 330 mm) are similar to those recently measured on the MEFOS machine (Figure 13, Reference 4).

One interesting aspect of the present computations is that solidification from the top (free) surface of the exiting strip shown in Figure 16 is predicted to take place downstream of the extended nozzle, such that an asymmetrical but two-sided solidification structure is indicated. This feature has also been observed in 10 mm strip cast at Lulea, an equi-axed structure about 60-70% of the strip height above the cooled substrate being observed. [4] In this respect, to describe a single-belt caster system as a one-sided strip solidification process is something of a misnomer.

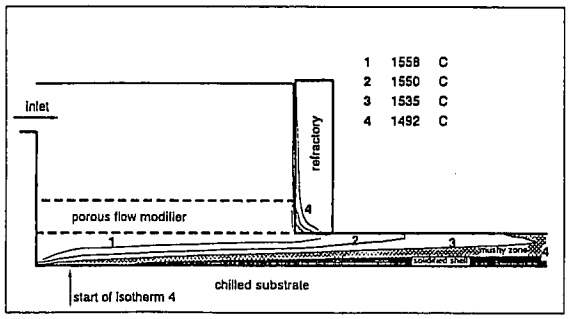

Fig 16. Predicted temperature isotherms (°C) for a flow-modified, extended nozzle delivery system.

However, our work also predicts that an extended nozzle concept, without the use of flow modifiers, can cause undesirable isotherms, as well as some remelting of a mushy (dendritic) zone in the exit region of the delivery system (Figure 17).

One encouraging feature of these predictions is the location of the start of the solidus isotherm. As seen, solidification takes place away from the meniscus region located between the moving belt and the entry wall. Similarly, by matching the belt speed with the steel's mean exit velocity ($\sim \sqrt{2gh}$) surface waves, such as hydraulic jumps, can be avoided, to assure good upper surface characteristics.

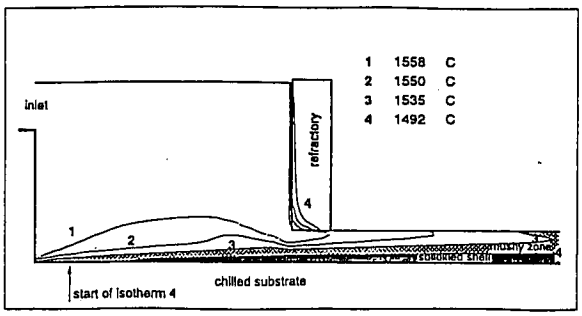

Fig 17 Predicted temperature isotherms(°C) illustrating the locations of solidus and liquidus boundaries for an extended-nozzle metal-delivery system.

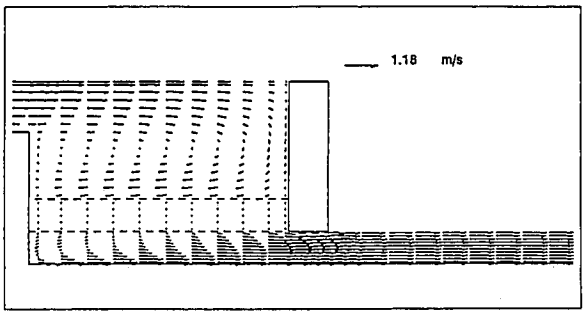

Fig 18. Predicted flow field (m/s) in the extended-nozzle region of a direct steel casting system, illustrating the elimination of short-circuiting through use of a reticulate flow modifier.

The predicted flow field in Figure 18, shows how one can avoid undesirable remelting features that are associated with the short-circuiting of liquid entering directly into the exit slot, by using a flow modifier, such as a 40 ppi reticulate medium (e.g., ZrO_2 filter). These fluid-flow predictions have been confirmed through the use of water models, and demonstrate how high-velocity strip-casting systems can be designed to perform under laminar-like flow conditions by presenting low-velocity liquid metal normal to a rapidly moving substrate. [1] Similarly, the computations suggest that these flows can be effected in a friction-free manner, if moving side-dams are used in conjunction with such extended nozzle delivery systems.

5.3 Heat Fluxes to Horizontal Substrates

In order to evaluate heat fluxes to variously coated steel belt substrates, the model testing equipment fitted with embedded thermocouples and shown in Figure 19 was constructed. Using the inverse heat transfer code developed, Figures 20 a and b show the instantaneous heat fluxes experienced when molten aluminum was fed onto the flame-sprayed coated steel bars, moving at commercial speeds in the order of 1 m/s. As seen from Figures 20 a and b, the instantaneous heat fluxes rose rapidly then fell sharply away as the freezing metal exited the mould and presumably released from the substrate. The data demonstrates the importance of actual plant experiments in determining appropriate boundary conditions for the various types of metal delivery/substrate permutations available to machine designers.

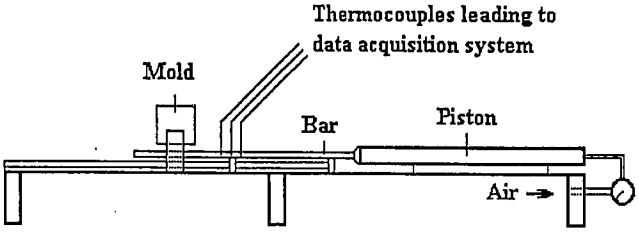

Fig 19. Schematic of the experimental apparatus.

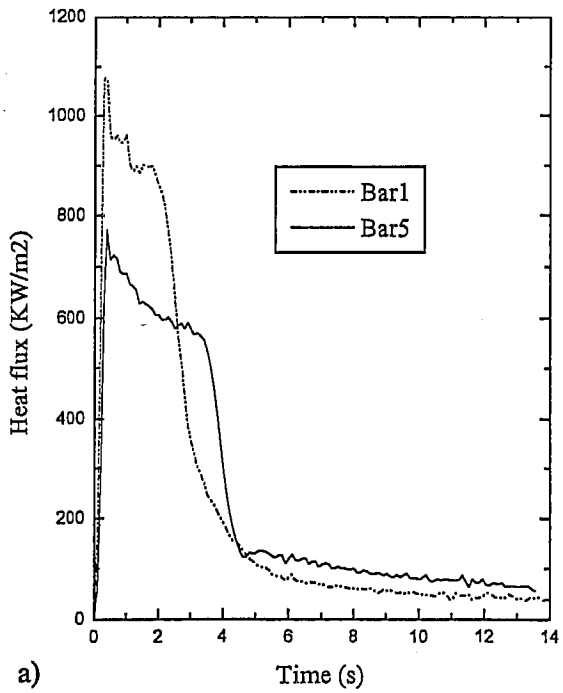

a)

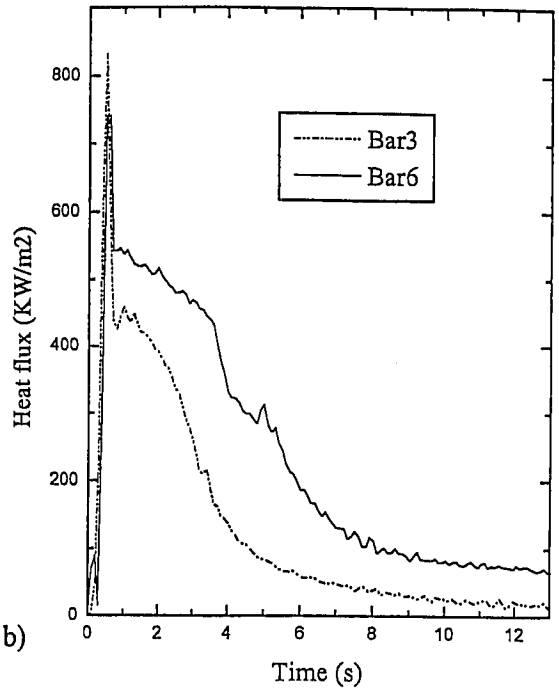

b)

Fig 20. Variation of heat flux with time for different substrate coatings. Lab scale apparatus for horizontal casting.

6. CONCLUSIONS

Thin strip casting has now become a commercial reality for stainless steels with the twin drum caster developed by Nippon Steel and Mitsubishi Heavy Industries. The present work demonstrates the value of computational fluid dynamics in determining optimum liquid metal delivery systems for such machines and shows the intrinsic superiority and need for a vertical slot nozzle over the bifurcated nozzles associated with conventional slab caster operations. This superiority derives from the predicted uniformity in shell growth across the width of the caster with such a delivery system.

In the case of horizontal single belt casting machines, it is suggested that the potential productivities to be derived from such casters make them more suitable candidates than TRC for the high tonnages associated with low carbon steel strip. The design concepts associated with an extended liquid steel delivery system have been explored using physical and mathematical models, and suggest that the pressurized delivery of liquid steel normal to a cooling substrate moving at high speed under laminar flow like conditions is possible.

In practical terms, the measurement of heat flux boundary conditions to these substrates is shown to be highly position and time dependent.

Meaningful development studies need to include embedded thermocouple tests of the type described in this paper, for process design and optimization.

REFERENCES

Jefferies, C., 1995, "Modelling a Novel, Thin Strip, Continuous Steel Caster Delivery System", Ph.D. Thesis, McGill University.

Tanaka, S., 1993, "Current Developments in Thin Strip Casting for Stainless Steel", Keynote Address, *International Symposium on Strip Casting, Hot and Cold Working of Stainless Steels, 32nd Conference of Metallurgists, CIM*, Quebec City, Quebec.

Mizoguchi, S., 1994, "Process Fundamentals on Near Net Shape Casting of Steel", *Proc. Ethem T. Turkdogan Symposium on Fundamentals and Analysis of New and Emerging Steelmaking Technologies, ISS*, Pittsburgh, pp. 165-170.

Nyström, R., Burström, E., Reichelt, W. and Urlau V., 1994, "DSC — A High Productivity Concept for Strip Production of Steel", *Metec 94, 2nd European Conference on Continuous Casting*, Düsseldorf.

Herbertson, J. and Guthrie, R.I.L., "Continuous Casting of Thin Metal Strip", Canadian Patent 536533, March 3, 1992, and U.S. Patent 4,928,748, May 29, 1990.

Guthrie, R.I.L. and Herbertson, J., 1988, "A Novel Concept for Metal Delivery to a Thin Strip Caster", *Proc. Int'l Symposium on Casting Near Net Shape Products, TMS of AIME*, Honolulu, pp. 335-349.

Bennon, W.D. and Incropera, F.P., 1987, "A Continuum Model for Momentum, Heat and Species Transport in Binary Solid-Liquid Phase Change Systems- I. Model Formulation", *Int. J. Heat Mass Transfer*, Vol. 30, No. 10, pp. 2161-2170.

Patel, V.C., Rodi, W. and Scheuerer, G., 1984, "Turbulence Models for Near-Wall and Low Reynolds Number Flows: A Review", *AIAA Journal*, Vol. 23, No. 9, pp. 1308-1319.

Aboutalebi, M.R., Hasan, M. and Guthrie, R.I.L., 1995, "Coupled Turbulent Flow, Heat and Solute Transport in Continuous Casting Processes", *Metallurgical Transactions B*, Vol. 26B, No. 4, pp. 731-744.

Poirier, D.R., 1987, "Permeability for Flow of Interdendritic Liquid in Columnar-Dendritic Alloys", *Metallurgical Transactions B*, Vol. 18B, pp. 245-255.

Flint, P.J., 1990, "A Three-Dimensional Finite Difference Model of Heat Transfer, Fluid Flow and Solidification in the Continuous Slab Caster, *Steelmaking Conference Proceedings*, pp. 481-490.

Shyy, W., Pang, Y., Hunter, G.B., Wei, D.Y. and Chen, M.-H., 1993, "Effect of Turbulent Heat Transfer on Continuous Ingot Solidification", *Transactions of ASME – Journal of Engineering Materials and Technology*, Vol. 115, pp. 8-16.

Schneider, M. and Beckermann, C., 1995, "Simulation of Micro/Macrosegregation during the Solidification of a Low-Alloy Steel", *ISIJ International*, Vol. 35, No. 6, pp. 1300-1307.

Hamel, F.G., Wang, G.L., Turcotte, S.F., Dufour, M. and Nadeau, J.P., 1994, "Results of Vertical Twin-Roll Casting Trials of Low-Carbon Steels", *Second Canada-Japan Symposium on Modern Steelmaking and Casting Techniques*, pp. 279-292.

Kim, Y., Farouk, B. and Keverian, J., 1991, "A Mathematical Model for Thermal Analysis of Thin Strip Casting of Low Carbon Steel", ", *Transactions of ASME – Journal of Engineering for Industry*, Vol. 113, pp. 53-58.

Wang, S.M. and Kang, Y.H., 1995, "Analysis of Flow and Heat Transfer in Twin-Roll Strip Casting by Finite Element Method", *Transactions of ASME – Journal of Engineering for Industry*, Vol. 117, pp. 304-315.

Howe, A.A., 1988, "Estimation of Liquidus Temperatures for Steels", *Ironmaking and Steelmaking*, Vol. 15, No. 3, pp. 134-142.

Tavares, R.,P., 1997, "Mathematical and Physical Modelling of Twin Roll Casting Processes for Steel", Ph.D. Thesis, McGill University.

Jefferies, C., Hasan, M. and Guthrie, R.I.L., 1992, "A Coupled Fluid Flow and Heat Transfer Study for Planar Thin Strip Steel Casting Processes", *Proc. 10th Process Technology Conf., 2nd Int'l Symposium on Modelling in the Iron & Steel Industry, I.S.S. of AIME*, Toronto, pp. 355-363.

Netto, P.G.Q., Tavares, R.P. and Guthrie, R.I.L., 1997, "A Technique for the Evaluation of Instantaneous Heat Fluxes for the Horizontal Casting of Aluminum", Light Metals 1997 Métaux Légers Proceedings, Conference of Metallurgists of CIM, Sudbury, Ontario. (in press)